Study of water mass transfer dynamics in frescoes by dielectric spectroscopy

R. Olmi and C. Riminesi

Istituto di Fisica Applicata del CNR - Via Madonna del Piano 10, 50019 Sesto F.no (FI), Italy

Summary. — The knowledge of moisture content (MC) is essential for determining the state of preservation of various types of hand-work: from building materials, such as bricks and concrete, to objects of artistic value, in particular frescoes and mural paintings. In all the above, moisture is the primary source of damages, as it affects the durability of porous materials. Dielectric properties of porous materials are strongly affected by the presence of water, suggesting dielectric spectroscopy as a suitable non-invasive diagnostic technique. The development of a quantitative relationship between MC and permittivity requires to investigate the dynamics of water mass transfer in porous media, and to determine its effect on the dielectric properties. In this paper a coupled mass transfer/dielectric problem is introduced and solved numerically, based on a finite element model. Results are compared to experimental dielectric measurement performed on plaster samples by the open coaxial method. The application of the dielectric technique to frescoes monitoring is proposed, showing the results obtained in an on-site study.

PACS 77.22.-d – Dielectric properties of solids and liquids.
PACS 84.40.Dc – Microwave circuits.
PACS 89.20.Bb – Industrial and technological research and development.

1. – Introduction

Water is one of the main sources of damage for cultural heritage artifacts based on porous materials, such as frescoes and mural paintings, painted wooden tables, ancient paper and parchment. On frescoes, it has a direct effect consisting in the deterioration of the painted layer, in plaster detachment and other kinds of damage, and an indirect effect related to the emergence of soluble salts (nitrates, carbonates, etc.) on the surface of the material. The efflorescence of salts, *i.e.* their crystallisation on the wall surface, produces the well-known whitening of the painted layer and, eventually, its detachment.

The knowledge of the moisture content (MC) in such porous materials is therefore important for their preservation. Furthermore, restoration techniques usually require to

investigate the permeability of a material to water, in order to choose the proper intervention procedure. Fresco restorers, for example, are used to imbibe a small surface of the painting by means of moistened wooden-pulp and to observe how rapidly the surface dries up, with the objective of determining a *quantitative* measurement of subsurface MC, and a meaningful and reliable measure of the time constant of the drying process.

A number of different techniques for determining moisture in walls have been developed in the last ten years, using infrared thermography [1], gravimetric tools [2], electrical resistivity [3], microwaves [4], unilateral NMR [5]. Each technique has pros and cons, related to the investigated depth, accessibility, accuracy, repeatibility and reliability, invasivity of the measurement.

Of course, a diagnostic tool useful in the context of cultural heritage must be non-invasive and non-destructive, and its interaction with the material must be free of any potentially dangerous effect for the material under measurement. Dielectric spectroscopy can be eligible for that purpose, in fact: 1) dielectric properties of porous materials are quite sensitive to the presence of water; 2) contact, non-destructive and reliable measurements can be easily performed on solid materials [6].

Several techniques have been suggested using electromagnetic methods for determining the MC of materials [7], and semi-empirical formulas have been proposed for relating dielectric properties and MC [8]. None of those formulas is fully satisfying when applied to moistened building materials, such as mortar or bricks, and more knowledge is needed in order to develop a quantitative relationship between MC and permittivity.

A moistened porous material can be modelled, from a macroscopic dielectric point of view, as a binary mixture consisting of a bulk host material (which is a mixture itself) and water. In such a simplified model, the relationship between MC and permittivity ϵ depends on the relative volume fractions of host material and water, and it can be expressed in terms of well-known mixing formulas [9]. The dynamics of water mass transfer inside a porous material can be studied in terms of different diffusion theories [10], using different *driving* potentials such as the chemical potential, vapour pressure and moisture concentration. A solution of the diffusion problem in terms of the last one [11, 12], allows to easily relate the MC to permittivity, after some simplifying assumptions have been made.

The following section introduces the mass transfer model based on the moisture diffusion equation, specialising it to the problem of interest to us. Subsequently, the dielectric mixture problem is solved and a physical model for a suitable resonant dielectric probe is discussed. The results obtained by the coupled mass transfer/dielectric model, in terms of the resonant frequency shift, are finally compared to experimental outcomes.

2. – The theoretical framework

Let us consider the following experimental framework. A slab of a porous material, initially dry or homogeneously moistened at a reference level, is put in contact with a water-saturated material at a time taken as $t = 0$. Water contact is maintained with the bottom of the slab, while the lateral surface is kept insulated and the top surface is free to exchange mass with the environment. The dynamics of water mass transfer and loss from the sample involves essentially two mechanisms: evaporation from the free surface of the slab and diffusion through the pore matrix. The physics of moisture transport inside porous materials is a very complex problem, requiring in principle a detailed microscopic knowledge of the capillary network geometry inside the material, including the presence of dead-end pores, multiple pore connections and so on. A macroscopic model of the

porous medium can be developed by considering an average material, consisting in a homogeneous mixture of bulk solid material and air, with air partially or fully replaced by water during moistening.

Let us now consider a slab portion, *e.g.*, a cylindrical region inside the slab and extending from top to bottom. The dielectric properties of such a cylinder change with time, as MC changes due to the above mechanisms. The material inside the cylinder can be treated as a dielectric two-component mixture (dry material/water), whose permittivity depends on the relative volume fractions of material and water. Of course, this last assumption has to be experimentally verified. Such a permittivity can be evaluated, for example, by measuring the capacitance across the cylinder.

Finally, the time behaviour of capacitance can be explained in terms of the time variation of MC in the tested region. The following subsections will develop the mass transfer and dielectric models, allowing to set up the numerical model to be compared with the experimental results obtained moistening a plaster sample.

2.1. *The moisture diffusion model.* – A macroscopic description of moisture dynamics in a capillary-porous material involves the solution of a differential transport equation written in terms of a water "driving potential" [13]. Restricting ourselves to the simplified assumption of isothermal moisture transport, such a potential can be the moisture concentration gradient, or the gradient of vapour pressure, or the chemical potential (Gibbs free energy), the choice depending on the peculiar characteristics of the problem at hand.

Having in mind the objective of developing a dielectric model, consisting of a mixture of solid dry material and water and depending on their relative volume fractions, the choice of the moisture concentration gradient appears the natural one. Denoting by θ the water volume concentration ($m^3 m^{-3}$) and by $\vec{m}$ the volumetric moisture flux ($m^3 m^{-2} s^{-1}$), Fick's first law is written in terms of a *moisture diffusivity D* having dimensions $m^2 s^{-1}$:

$$\vec{m} = -D\nabla\theta. \tag{1}$$

From the water content balance in an elementary test volume, eq. (1) brings to the following non-linear equation for water volume concentration:

$$\dot{\theta} = \nabla\left(D\nabla\theta\right), \tag{2}$$

where $\dot{\theta}$ denotes the time derivative of θ, as usual. Water concentration θ represents both liquid water and aqueous vapour and (2) is a good approximation in usual conditions of temperature/pressure, with the diffusivity coefficient D taking into account both liquid flow and vapour diffusion [12]. We assume an exponential dependence of the diffusivity D on the volumetric MC θ, via a parameter β to be experimentally determined, as suggested by [14]:

$$D = D_0 \exp[\beta\theta]. \tag{3}$$

The following mass transfer problem is analysed. A porous material, like mortar, is initially at a given constant volumetric MC θ_0. In the following, we shall refer to a tile of mortar having a square cross-section, as shown in fig. 1. At time $t = 0$ the bottom surface of the tile is put in contact with an ideal reservoir of water, allowing a fast
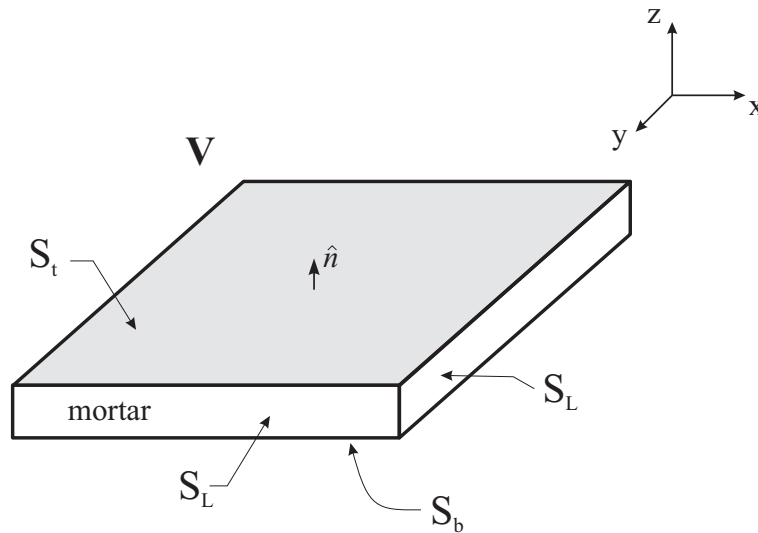
Fig. 1. – The geometry of the moisture transport problem.

mass exchange with mortar. In practice, a bed of water-saturated cotton wool can be reasonably approximated by such an ideal condition, as the diffusivity of cotton wool is orders of magnitude greater than that of mortar-like materials. So, the initial and boundary conditions inside mortar and on its external surface are

$$
\begin{aligned}
\theta(\vec{r},0) &= \theta_0, & \vec{r} &\in V, \\
\nabla\theta(\vec{r},t) \cdot \hat{n} &= 0, & \vec{r} &\in S_L, \\
\theta(\vec{r},t) &= \theta_b, & \vec{r} &\in S_b, \\
\nabla\theta(\vec{r},t) \cdot \hat{n} + h\theta(\vec{r},t) &= f, & \vec{r} &\in S_t.
\end{aligned}
\tag{4}
$$

The above conditions express the following physical situation: a) the lateral surface S_L is insulated; b) the bottom surface S_b is subjected to an ideal water influx, represented by a Dirichlet boundary condition; c) the top surface S_t exchanges water (in vapour phase) with the environment. A proportionality between water flux and the concentration θ at the material surface is assumed in c) by analogy with thermal problems that are governed by the same diffusion equation. $\hat{n}$ denotes the outward normal at the material/air interface. The last condition of (4) requires the exchange coefficient h to be determined experimentally. The f function depends on several parameters (such as the relative humidity of the environment, the saturated water vapour pressure, and more), but it can be assumed to be given by a constant value, *i.e.* $f = h\theta_a$, with θ_a depending on the relative humidity of the environment.

Choosing an elementary volume (EV) V_e inside the material, the water volume concentration θ is the ratio between the volume of water V_{ew} inside the EV and its total volume: $\theta = V_{ew}/V_e$. Water is assumed to be mainly in the liquid phase inside the material. Denoting by ρ_w and ρ the densities of liquid water and of the host material, respectively, the mass of a volume of material containing N EVs is given by

$$
M_m = N\rho V_e.
\tag{5}
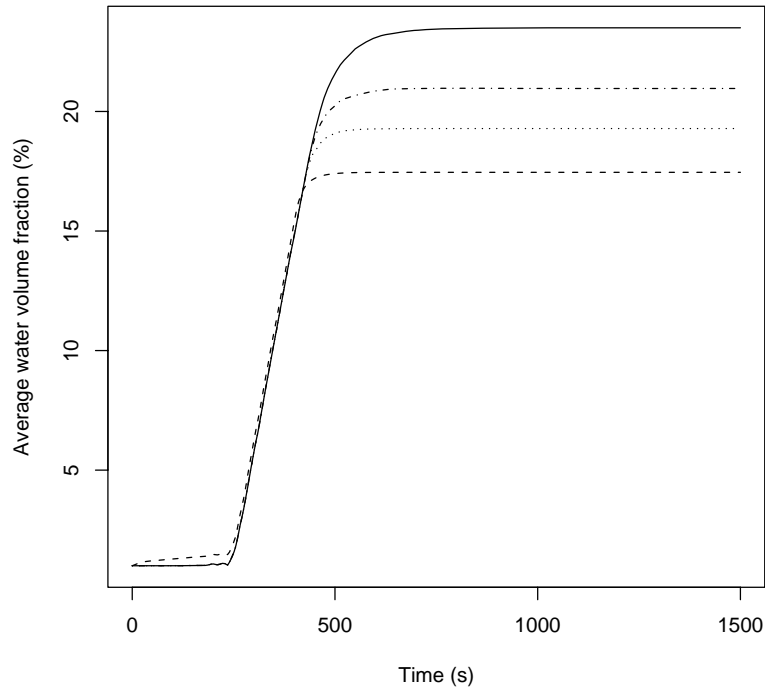$$

Fig. 2. – Results of FEM mass transfer simulation for different exchange coefficients h: $10^4 \, \mathrm{m}^{-1}$ (dashed line), $10^2 \, \mathrm{m}^{-1}$ (dotted line), $20 \, \mathrm{m}^{-1}$ (dot-dashed line), 0 (solid line).

When water is present inside the material, it substitutes a volume fraction θ that was occupied by air, thus the mass of water inside the material is

$$\text{(6)} \qquad\qquad M_w = N\rho_w \theta V_e \,.$$

The mass of the moistened volume is therefore $M'_m = N(\rho + \theta\rho_w)V_e$ and the moisture content (defined on wet basis), given by $\Psi = M_w/M'_m$, is related to the moisture volume concentration θ by

$$\text{(7)} \qquad\qquad \Psi = \frac{\rho_w \theta}{\rho + \rho_w \theta} \,.$$

If the material is modelled as a homogeneous and isotropic distribution of EV's, θ corresponds to the relative volume fraction of water inside the material, while $1 - \theta$ is the volume fraction of host material. This last consideration will be used for building the dielectric model, as described in the following section.

A finite-element (FE) model implementing eq. (2), with the proper initial and boundary conditions (4), has been set up. The geometry of the model is shown in fig. 1: it consists of a single layer of thickness 2.3 cm, having the physical characteristics of mortar: $D_0 = 2.35 \times 10^{-10} \, \mathrm{m}^2 \, \mathrm{s}^{-1}$, $\beta = 35.0$.

To get an idea of the dynamics of moisture transport, fig. 2 shows the parameter θ, averaged on a slab of thickness 0.5 cm from the top surface (*i.e.* on the opposite side with

respect to that experiencing the water inlet), for four different exchange coefficients h: $10^4 \, \mathrm{m}^{-1}$ (dashed line), $10^2 \, \mathrm{m}^{-1}$ (dotted line), $20 \, \mathrm{m}^{-1}$ (dot-dashed line), 0 (solid line), the last corresponding to "insulation".

2˙2. *The dielectric model*. – Subsection **2**˙1 describes how to compute the volume fraction of water $\theta(\vec{r}, t)$ wherever in the host material, at any time. Given $\theta(\vec{r}, t)$ the permittivity of the material can be computed at any $(\vec{r}, t)$ by means of one of the formulae developed for mixtures [9], with the implicit assumption that such a permittivity refers to a small—but macroscopic—volume of material positioned at $\vec{r}$. An EV, as defined for the moisture diffusion problem, can be a meaningful choice for such a volume.

As is well known, the mixing rules depend on several factors, first of all the shape of the inclusions, and a unique formula can be devised only for regular, simple geometries. Nevertheless, given the two components ϵ_m and ϵ_w of the binary mixture material/water, dielectric bounds for the *effective dielectric constant* ϵ_e can be rigorously determined, such as those introduced by Hashin and Shtrikman [15]:

$$(8) \qquad \epsilon_{e1} = \epsilon_m + 3\theta \left[\epsilon_m (\epsilon_w - \epsilon_m) \right] / \left[\epsilon_w + 2\epsilon_m - \theta(\epsilon_w - \epsilon_m) \right],$$
$$\epsilon_{e2} = \epsilon_w + 3(1 - \theta) \left[\epsilon_w (\epsilon_m - \epsilon_w) \right] / \left[\epsilon_m + 2\epsilon_w - (1 - \theta)(\epsilon_m - \epsilon_w) \right].$$

The effective dielectric constant of the mixture must be between the above two bounds. Once the time behaviour of $\theta(\vec{r})$ is known, a meaningful dielectric constant for the mixture can be computed at any time and space location by means of one of the mixing formulas available in the literature. It will be shown that a reasonable choice is a modified version of the Sen formula [16], frequently employed for rocks and soils:

$$(9) \qquad \frac{\epsilon_e(\vec{r}, t) - \epsilon_m}{\epsilon_w - \epsilon_m} = \theta(\vec{r}, t) \left[\frac{\epsilon_e(\vec{r}, t)}{\epsilon_w} \right]^{\alpha},$$

where α, the de-polarisation factor of the inclusion, can be adjusted to fit the experimental data. It is exactly $1/3$ for spherical inclusions, and can be any value between 0 and 1 for arbitrary shapes.

The average dielectric constant of plaster samples has been experimentally determined by using the open-coaxial technique [6]. Figure 3 shows the open-coaxial measurement set-up used for the experiments.

The set-up of fig. 3 is simulated by means of a FEM model, implementing the electromagnetic (EM) problem of a section of coaxial line terminating on a slab of plaster material. The measuring coaxial line is excited in its fundamental TEM mode, and the reflection coefficient Γ at the coaxial aperture is the quantity to be computed. The determination of Γ involves the solution of a full-wave EM problem, requiring to match the coaxial line fields—expressed in the most general case as a sum of the dominant mode and a doubly-infinite set of transverse magnetic (TM) and transverse electric (TE) modes—with the diverging EM field at the aperture. By symmetry considerations, no longitudinal magnetic field can be expected at the interface between probe and material, *i.e.* the EM field is TM to the axis of the coaxial line and it can be computed in terms of a scalar potential, consisting in the angular component of the magnetic field H_ϕ. The equation to be solved is, therefore,

$$(10) \qquad \nabla \times \left(\frac{1}{\hat{\epsilon}} \nabla \times H_\phi \right) - \mu_r k_0^2 H_\phi = 0,$$
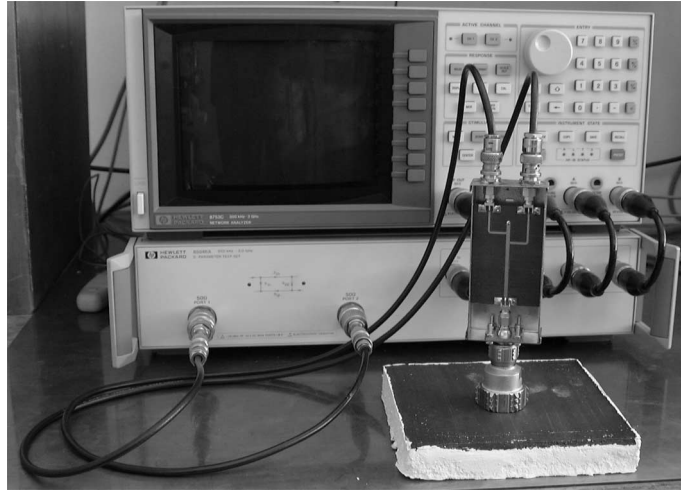
Fig. 3. – The measurement set-up.

where $\hat{\epsilon}$ is the complex permittivity in the various materials (*i.e.* inside the coaxial and in the plaster slab), k_0 is the free-space wave number and μ_r the relative magnetic permeability, equal to 1 for ordinary non-magnetic materials.

The reflection coefficient Γ is computed in terms of the field at the aperture plane and of the incident TEM field. Once Γ is known, the admittance at the coaxial aperture can be computed:

$$(11) \qquad Y_a = Y_0 \frac{1 - \Gamma}{1 + \Gamma},$$

where Y_0 is the reciprocal of the characteristic impedance of the coaxial line. The aperture admittance can be represented as a lumped circuit consisting of a parallel between a frequency-dependent conductance G_a and a capacitance C_a. This last parameter, also frequency dependent, allows to compute the relative dielectric constant:

$$(12) \qquad \epsilon_r' = \frac{C_a(f)}{C_0(f)}.$$

$C_0(f)$ is a geometrical factor, nearly frequency independent in the frequency range of interest, consisting in the capacity of the open coaxial facing air. The dielectric constant (12) is an average over the volume where the electric field lines mainly develop themselves. The size and shape of such a volume can be computed, for example, as described in [17].

Actually, the measuring probe consists of a microwave resonator terminating on an open-coaxial probe, and the termination capacity, containing all information about the permittivity of the material under measurement, is obtained by measuring a resonant frequency shift with respect to the sensor in air. The resonant probe is fully described elsewhere [18]. For a given material, ϵ_r' is a function of frequency, but it happens to be nearly constant in the microwave range where the resonant coaxial sensor operates (about 0.9–1.4 GHz).
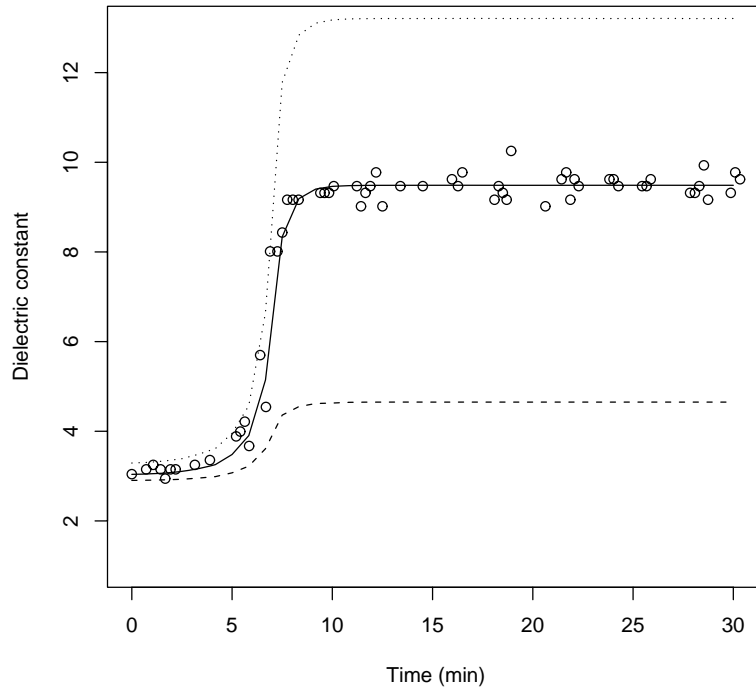
Fig. 4. – Comparison between measured (circles) and computed (solid line) average dielectric constant. Dashed and dotted curves refer to lower and upper Hashin-Shtrikman bounds, respectively.

2.3. *The coupled mass transfer/dielectric problem*. – Equation (2), with initial and boundary conditions given by (4), gives a time-dependent water volume fraction $\theta(t)$ which, in turn, makes the mixture dielectric constant (9) a time-dependent quantity. Therefore, the EM problem represented by eq. (10) must be solved at each time value, making the volume-averaged relative dielectric constant (12) a function of time.

Figure 4 shows the time behaviour of $\epsilon_r(t)$, computed at 1 GHz, during moistening. Solid line refers to $\epsilon_r(t)$ computed by the FEM model, using (9) with $\alpha = (2.7)^{-1}$. The experimental points are represented by circles in fig. 4, while dashed and dotted lines represent the average dielectric constant values computed from $C(t)/C_0$ using the Hashin-Shtrikman bounds (8). $C(t)$, the capacitance of the loaded open-coaxial probe, is a function of time via $\epsilon'_r(t)$.

The experiment referred by fig. 4 concerns the moistening of a tile of mortar having the geometry of fig. 1. The tile, shown in fig. 3, has dimensions $14.7 \times 14.7 \times 2.3$ cm, and a dry weight of 865.1 g. Water is absorbed from bottom only (the lateral surface is impermeable) through a moistened cotton bed. The initial temperatures of the tile, cotton and environment are 24.1 °C. The final (saturation) weight of the tile is 974.8 g, corresponding to a volume fraction of 0.23.

3. – Application

Figure 4 shows the time behaviour of the average dielectric constant, computed as described in the previous section, during the diffusion of water inside the material. The
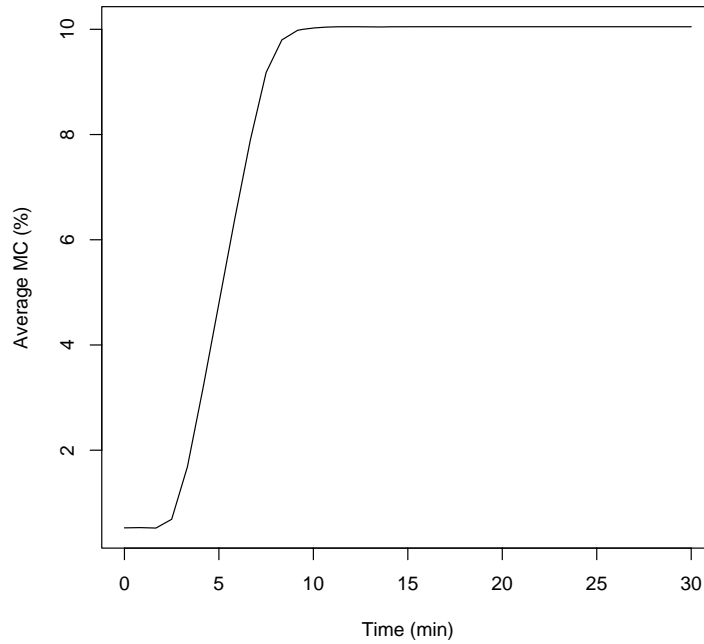
Fig. 5. – Time behaviour of the average MC during moisture diffusion.

peculiar characteristics of the open-coaxial dielectric measurements are such that the size of the *probed* region, *i.e.* the region of space where the electric field lines mainly develop themselves, is nearly semi-spherical with radius approximately equal to the width of the coaxial aperture [17], *i.e.* of the order of 1 cm. It therefore appears reasonable to choose such a volume as a reference for computing the average moisture content of the material. Such an average MC, computed according to eq. (7), is reported in fig. 5 as a function of time.

Actually, the maximum depth of the measurement can be substantially greater (up to 2-3 cm) depending on the wetness of the material, as has been experimentally verified on metal-backed plaster tiles of increasing thickness. However, the sensitivity of the measurement falls off with depth, making the above average depth a significant figure.

The similarity between the time behaviour of the average dielectric constant and the average MC is evident from the two figures, suggesting a quasi-linear relationship between the two quantities.

The dielectric constant, however, is not a primary quantity, because it is derived by means of a model from the relative frequency shift $\Delta f_r = (f_0 - f)/f_0$, where f_0 is the resonance frequency measured in air. It is therefore useful to relate directly Δf_r—which is a measured quantity—to the moisture content. The resonator, described in [6], consists in a short-circuited section of transmission line of characteristic impedance Z_0 and wave number β, of length d, terminated by a capacitance C which, by (12), is a function of ϵ_r'. The resonance condition is

$$(13) \qquad Z_0 \tan(\beta d) = \frac{1}{2\pi f C} .$$

The relation between Δf_r and ϵ'_r is obtained manipulating (13). After some approximation, Δf_r can be put in the following form:

$$(14) \qquad \Delta f_r = 1 - \frac{a}{\epsilon'_r + b} = \frac{\epsilon'_r + c}{\epsilon'_r + b}$$

with a, b and c suitable constants, and $c < b$.

The dependence of the dielectric constant ϵ'_r on the moisture content Ψ involves a parabolic relation, at least in the range of MC we are interested in

$$(15) \qquad \epsilon'_r = \alpha + \beta\Psi + \gamma\Psi^2$$

with α, β and γ suitable constants.

By inserting (15) into (14) the desired relation between Δf_r and the MC is obtained. Δf_r happens to be a rational function of Ψ:

$$(16) \qquad \Delta f_r(\Psi) = \frac{P_1(\Psi)}{P_2(\Psi)} = \frac{\alpha_1 + \beta\Psi + \gamma\Psi^2}{\alpha_2 + \beta\Psi + \gamma\Psi^2}$$

with P_1 and P_2 both second-order polynomials, as shown in (16). $\Delta f_r(\Psi)$ has unitary asymptotic value and it is monotonically increasing because $\alpha_2 > \alpha_1$ by (14). For plaster material, and for $\Psi \in [0, \Psi_s]$ (where Ψ_s denotes the saturation MC), Δf_r is a nearly linear function of the MC, as shown in fig. 6. This kind of linear relation has been experimentally confirmed.

Figure 6 shows Δf_r computed solving eq. (13) using the modified Sen expression for the permittivity of the binary mixture between dry plaster and water representing the moistened plaster. Dry plaster dielectric properties are assumed frequency independent, $\hat{\epsilon}_m = 3.2(1 - 1.4 \times 10^{-2}i)$, whilst water permittivity is assumed to exhibit a single-relaxation Debye dispersion:

$$(17) \qquad \hat{\epsilon}_m = \epsilon_s + \frac{\epsilon_\infty - \epsilon_s}{1 + i\omega\tau} - i\frac{\sigma}{\omega\epsilon_0} \, ,$$

where a ionic conductivity term σ is added to investigate how the presence of salts dissolved into water influences the measured parameter Δf_r. The other parameters customarily denote the low- and high-frequency dielectric constants (ϵ_s and ϵ_∞, respectively), the relaxation time (τ) and the permittivity of vacuum (ϵ_0).

A solution of calcium nitrate, $Ca(NO_3)_2 4H_2O$, in water is considered, as efflorescence of this kind of salt rather commonly develops on frescoed walls. With reference to fig. 6, circles concern a ionic conductivity of $0.4\,S/m$, while crosses refer to a conductivity of $10\,S/m$. The first value represents a very low salt concentration (well below $0.05\,mol/l$), the second is the conductivity at $1\,GHz$ of a $2\,mol/l$ solution, a value close to saturation (calcium nitrate solubility is about $380\,g/l$).

The influence of ionic conductivity on the parameter Δf_r appears negligible, confirming the suitability of dielectric spectroscopy for measuring the sub-superficial moisture content in a porous material. The method has several peculiar characteristics (high sensitivity, non-invasivity, reliability, portability) that make it eligible for the diagnostics of fresco paintings, as shown in the examples reported in the following section.
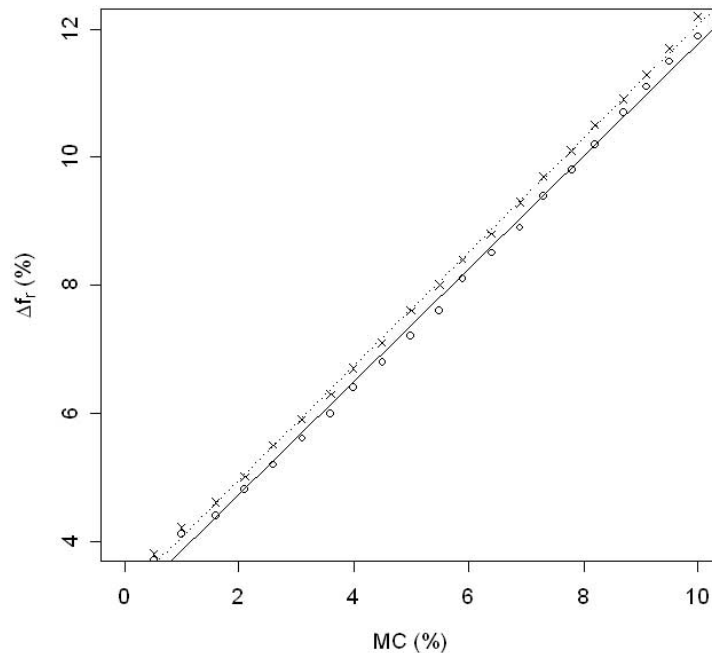
Fig. 6. – Relationship between Δf_r and MC.

3˙1. *In situ monitoring examples.* – Dielectric spectroscopy has been applied as a diagnostic technique in the vary last years on several frescoes in churches and museums in Florence, Rome and other places, in cooperation with the Opificio delle Pietre Dure of Florence and with the Istituto Centrale per il Restauro of Rome. Two cases are presented as an example of the results that can be obtained by the technique.

The first case refers to the monitoring of moisture content in a fresco in the Basilica of San Clemente in Rome. The Basilica of San Clemente consists of three levels, making it a unique case in Italy. The middle level, built starting from the fourth century, contains several ancient frescoes—including *The legend of St. Alexis* and *St. Clement at mass and the legend of Sisinnius*—whose conditions are rapidly deteriorating, probably due to the moisture diffusion from the floor. Indeed, the middle level of the Basilica rests on subterranean I century buildings, and is itself below the street level, making it a very humid environment. The monitoring of the above frescoes began two years ago, in preparation of a drilling campaign that will be carried out in the next future with the purpose of reducing moisture diffusion from the floor to the frescoed walls.

Figure 7 shows a contour map and a vertical profile of the subsurface MC measured on the fresco "The legend of St. Alexis" in October 2007. Each subdivision on the vertical axis equals 30 cm; those on the horizontal axis equal 40 cm. Measurements have been taken at the cross-points between the labelled horizontal and vertical lines. Both graphs point out the existence of a gradient in the MC. Both the vertical profile, measured on the right side of the wall with the fresco, and the front profile show that MC decreases from a value between 8 and 9% at the bottom of the fresco to an average value of about 5% rising up.
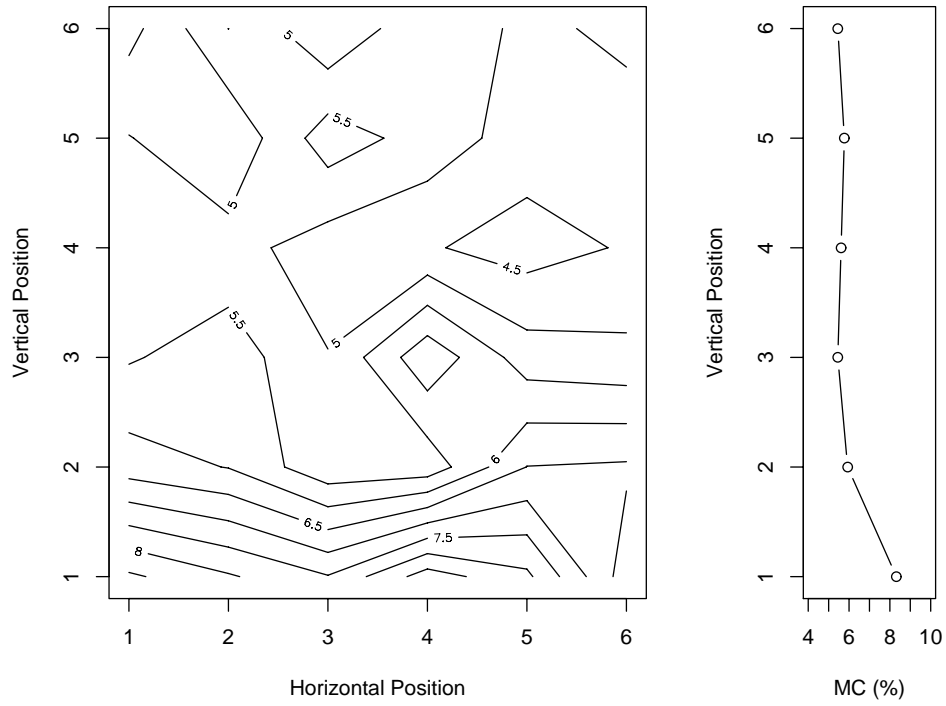
Fig. 7. – Moisture content map (on the left) on the Sant'Alessio fresco in the Basilica of San Clemente, and the lateral vertical profile (on the right).
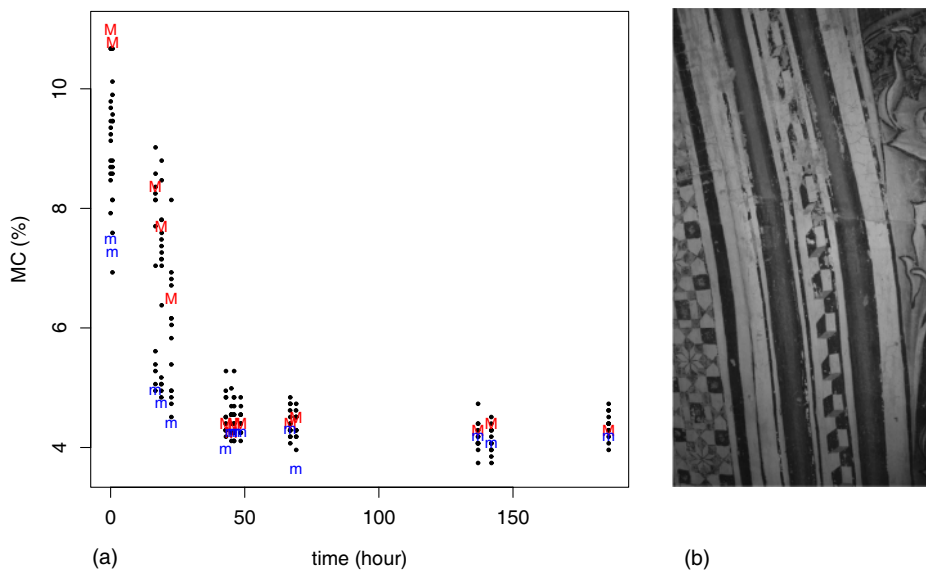

Fig. 8. – Moisture diffusion dynamics (a) on a fresco in the Church of Santa Croce (b).

The second case concerns an investigation of the dynamics of moisture diffusion in a frescoed wall of the Church of Santa Croce in Florence. Restorers use an absorbing *poultice* for extracting soluble salts from a wall. The poultice, consisting in a very wet mixture of cellulose pulp with sand or other materials capable of absorbing water, is placed on a fresco—usually separated from the painted layer by a sheet of *Japanese paper*—for some hours or days. In the case reported in fig. 8, the MC has been recorded during time on 15 points lying on the vertical line identified by the white rectangles in the central region of fig. 8(b). The points "M" and "m", in fig. 8(a), respectively refer to the maximum and minimum initial value of the MC, immediately after having removed the absorbing poultice. MC has been monitored for about 170 hours, up to the restoration of moisture equilibrium with the environment (MC between 4 and 5%). This kind of time-dependent monitoring is possible thanks to the real-time response of the dielectric measuring system.

The accuracy of on-site measurements depends on the flatness of the wall surface: a circular flat region with a diameter of about 3 cm is sufficient to insure maximum accuracy. A moderate roughness does not degrade the measurement. The method is highly reproducible and reliable, and the accuracy, estimated on laboratory samples, is of the order of 0.1%. The dielectric measurement is not actually density independent, although the permittivity of building materials (mortar, plaster, bricks, rocks) are quite similar and very different to that of water. A simple calibration procedure on a particular material (involving only a measurement on a dry sample and on a water-saturated one) is however recommended when absolute, high-precision measurements are needed.

4. – Conclusions

Dielectric spectroscopy has been demonstrated to be capable of measuring the moisture content of porous materials such as plaster, which is the base material of *intonaco* on which ancient frescoes were painted. A technique based on dielectric spectroscopy, using a resonant sensor operating in the microwave range, has been demonstrated to allow reliable and highly reproducible measurements. The physical bases of the measurement method have been discussed, showing that the relative frequency shift of the resonator can be directly related to the moisture content, that the relation is nearly linear, and that it is almost independent on the presence of ionic conductivity. A mixed mass-transfer/dielectric model has been developed, which allows to determine the proper dielectric function for the mixture of plaster and water.

The technique has been applied in several *in situ* cases. Two particular cases have been selected and briefly discussed to show the usefulness of the method, concerning the monitoring of frescoes before or after a restoration intervention and the quantitative study of the dynamics of water absorption inside a frescoed wall.

* * *

REFERENCES

[1] Avdelidis N. P. and Moroupolou A., *J. Cult. Herit.*, **5** (2004) 119.
[2] Pamplona M., Meloa M. J. and Tiano P., *Proceedings of SMW08 In situ Monitoring of Monumental Surfaces* (EDIFIR, Firenze) 2008, pp. 247-253.
[3] Sass O. and Viles H. A., *J. Cult. Herit.*, **7** (2006) 257.
[4] Maierhofer C. and Wostmann J., *NDT&E Int.*, **31** (1998) 259.
[5] Sharma S., Casanova F., Wache W., Segre A. and Blumich B., *Magn. Reson. Imaging*, **21** (2003) 249.
[6] Olmi R., Bini M., Ignesti A. and Riminesi C., *Meas. Sci. Technol.*, **11** (2000) 1623.
[7] Kraszewski A., *Microwave Aquametry* (IEEE Press, New York) 1996.
[8] Meyer W. and Schilz W. M., *IEEE Trans. Microwave Theory Tech.*, **29** (1981) 732.
[9] Sihvola A., *Electromagnetic mixing formulas and applications*, *IEE Electromagnetic Wave Series 47* (The Institution of Electrical Engineers, UK) 1999.
[10] Alvarez C. A., *Evaluation of moisture diffusion theories in porous materials*, Doctor Thesis, Mechanical Engineering, Virginia Polytechnic Institute and State University (1998).
[11] Pel L., Kopinga K., Bertram G. and Lang G., *J. Phys. D: Appl. Phys.*, **28** (1995) 675.
[12] Pel L., *Moisture transport in porous building materials*, PhD Thesis, Technische Universiteit Eindhoven (1995).
[13] Galbraith G. H. and McLean R. C., *Proceedings of IBPSA Conference Building Simulation, 1997*, pp. 351-354, see `www.IBPSA.org`.
[14] Gardner W. R. and Mayhugh M. S., *Soil Sci. Soc. Am. Proc.*, **22** (1958) 197.
[15] Hashin Z. and Shtrikman S., *J. Appl. Phys.*, **33** (1962) 3125.
[16] Sen P. N., Scala C. and Cohen M. H., *Geophysics*, **46** (1981) 781.
[17] Hoshina S., Kanai Y. and Miyakawa M., *IEEE Trans. Magn.*, **37** (2004) 3311.
[18] Olmi R., Bini M., Ignesti A., Priori S., Riminesi C. and Felici A., *Meas. Sci. Technol.*, **17** (2006) 2281.